Steady and transient performance of a pump-turbine on an open-loop test rig: pump mode

AUTHOR(S)

J H Hu, J D Yang, Wei Zeng

PUBLICATION DATE

01-01-2018

HANDLE

10536/DRO/DU:30164563

Steady and transient performance of a pump-turbine on an open-loop test rig: pump mode

IOP Conf. Series: Earth and Environmental Science **163** (2018) 012082 doi:10.1088/1755-1315/163/1/012082

Steady and transient performance of a pump-turbine on an open-loop test rig: pump mode

J H Hu[1], J D Yang[1] and W Zeng[2]

[1] State Key Laboratory of Water Resources and Hydropower Engineering Science, Wuhan University, Wuhan 430072, China
[2] School of Civil, Environmental and Mining Engineering, University of Adelaide, SA 5005, Australia

jinhonghu@whu.edu.cn

Abstract. In order to study steady and transient characteristics of the pump turbine, a model pumped storage system was established in State Key Laboratory of Water Resources and Hydropower Engineering Science, Wuhan University. Different from typical closed-loop test rigs, this open-loop system has a constant upstream and downstream water level, two parallel pump-turbines, surge tank, power grids, etc., to achieve similar operating modes as in prototype power station. This paper aims to investigate the pump performance of the pump-turbine unit, including steady state and transient state. The structure of the present paper is organized as follows: 1) Steady pump performance of a model pump-turbine under three guide vane openings (GVO) was obtained by point-by-point measurements with the the adjustment of spherical valve; Meanwhile, the source of steady hysteresis as well as hump instabilities was identified by pressure analysis. It was found that the pressure instabilities in draft tube caused the drop in the energy performance curve as well as the hysteresis. 2) By dynamically adjusting the opening of the spherical valve, performance curves from nominal flow discharge to zero discharge were obtained under a constant GVO. The results showed that the performance curves of the torque and the efficiency could be measured in a quasi-steady way with sufficient switch time of the spherical valve, despite a clear dynamic loop of the energy performance curves. 3) The performance curves of a model pump-turbine were extended from high flow discharge region to nominal flow discharge operating point through a transient experiment in which the head varied.

1. Introduction

Pumped storage units can operate in two modes, which make it feasible to change operating condition to response to the need of the grid. However, when operating in part load conditions in pump mode, the unit could be unstable. At the same time, the discharge-energy performance curve of the pump-turbine unit displays a hump-shaped region. In order to improve the understanding of this phenomenon, pressure measurement [1], flow observation [2,3,4], velocity measurement [5,6,7,8] were utilized by researchers. In addition, 3-D numerical simulations were conducted to investigate instability caused by flow pattern [9,10,11]. It was shown that the hump characteristics are not only related to the separation of the inlet flow of the pump-turbine, but also with rotation stalls in cascades.

This paper reports steady and transition experiments conducted on an open-loop model test with a pumped storage system. By the adjustment of the opening of the spherical valve, performance curves

in pump mode from nominal operating point to zero flow discharge point were obtained through steady point-by-point measurements in flow decreasing direction as well as flow increasing direction. The hump-shaped and hysteresis characteristics of the performance curves could be observed in part flow conditions. The reason for hump phenomena and hysteresis characteristics were discussed through analysis of global characteristics and pressure pulsation. Subsequently, the results of two types of transient experiments were presented. First, the spherical valve was continuously operated to acquire the performance curves in part flow conditions dynamically. Dynamic performance curves of three sets of spherical valve closing/opening time were compared. Second, the transient tests with a spontaneous method to vary head were carried out to obtain the performance curve in high flow discharge condition. Finally, the factors that influence the experimental precision were discussed.

2. Experimental Setup

The sketch of the pumped storage model system in Wuhan University was shown in figure 1, including 2D and 3D view. Circulating pump delivered water from underground reservoirs to the upstream and downstream reservoirs. The water level in the upstream and downstream was maintained constant through overflow. The whole system was designed with IEC60193 [12] and ensured that experiments were conducted with no occurrence of cavitation.

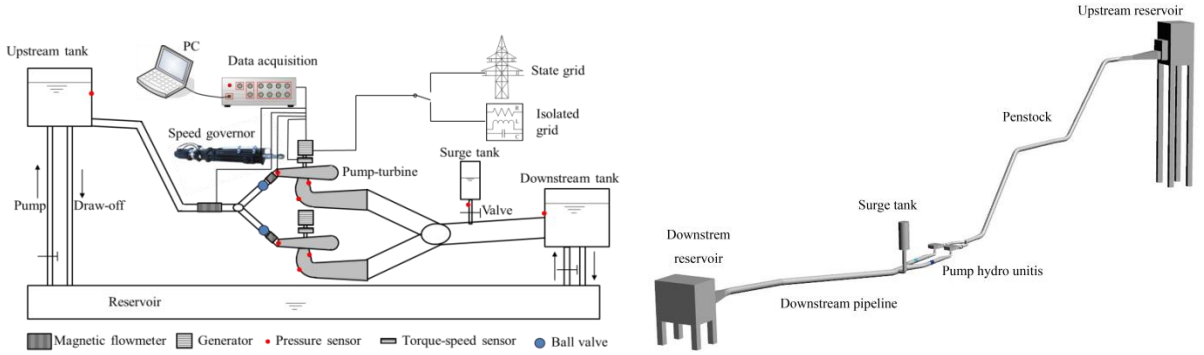

Figure 1. Model pipe system

In steady state operations, the infinite power grid ensured that the rotational speed of the unit is stable. Because the whole system was scaled according to the real power station, the piping system was more than 50 m. Besides, in the downstream of the unit, a model surge tank was established. In transient operations such as emergency load rejection, the rotational speed of the unit can rise up to 135% of the nominal value.

In table 1, geometrical parameters and rated operating parameters of the model unit were presented. There were two model runners on the test rig, whose characteristics are quite different in turbine braking mode but similar in designed operating conditions. Runner A, with gentle S-shaped characteristics, was selected for the experiment of this paper. The other unit was not in operation during experiments. Table 2 displays sensors used to measure mechanical and flow parameters. Table 3 and figure 2 illustrate the location of the two pressure sensors. For the measurement of pressure in spiral case and draft tube cone, Micro MPM absolute pressure sensors calibrated with Fluke 754 were used. The PCB dynamic pressure sensors, calibrated by the manufacturer，were used to measure the pressure pulsations in the vaneless region as well as in the guide vane channel.

The control of the spherical valve was of great importance in current tests. In steady tests, the hydraulic loss of the test rig was changed by adjusting the spherical valve, which was proposed by Doerfler [13] to maintain the stable operation of the prototype pump turbine in low GVOs. The physical mechanism of the operation can be explained by changing the system's characteristic curve by Landry [14] and increasing the resistance of the system by Nielsen [15]. This method has been employed to experimentally explore the steady-state performance of pump turbine in turbine brake

mode by Guggenberger [16]. For dynamic tests, the spherical valve was adjusted continuously closing or opening to obtain the dynamic performance curves in part flow condition.

Table 1. Model unit parameters

N_{QE} ($m^{0.75}$ s^{-}	Inlet diameter	Outlet diameter(mm)	Guide vane height	Z_b	Z_g	Rated n (rpm)	Rated H (m)	Rated Q (L/s)	Full rotational
37.91	280	146.34	24.44	9	20	1000	10.54	49.1	66.4

Table 2. Specifications of the different sensors

Sensor type	Positions	Measurement range	Accuracy degree (%)	Linearity (%)	Uncertainty(%)	Signal
Pressure sensor (Micro MPM 480)	1# Spiral case inlet	0–200 (kPa)	0.25	0.052 F.S	0.109	4–20 mA
	1# Draft tube inlet	−20–50 (kPa)		0.035 F.S	0.083	
	2# Spiral case inlet	0–200 (kPa)		0.051 F.S	0.079	
	2# Draft tube inlet	−20–50 (kPa)		0.053 F.S	0.621	
Flow meter (KROHNE IFM 4110)	Upstream main pipe	−200–200 (L/s)	0.3	0.128 F.S	/	4–20 mA /Frequency
Flow meter (OPTIFLUX 2000)	1# branch pipe	−70–70 (L/s)	0.2	0.157 F.S	/	
	2# branch pipe	−70–70 (L/s)		0.141 F.S		
Torque sensor (HLD09)	Between 1# turbine and 1# generator	−100–100 (N.m)	0.2	0.040% F.S	/	4–20 mA /Frequency
	Between 2# turbine and 2# generator	−100–100 (N.m)		0.020% F.S		

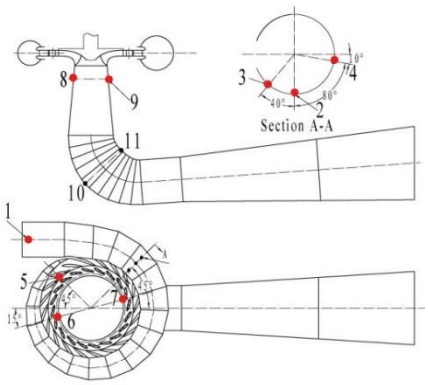

Figure 2. Location of pressure sensors

Table 3. Type and position of pressure sensors used in this paper

No.	Sensor type	Position
1	MPM 480	Spiral case inlet
5	PCB 112A	stay vane
6	PCB 112A	Vaneless space 1
8	MPM 480	Draft tube inlet 1

3. Results and discussions

In both steady and transient tests, the sampling rate was kept 1000Hz. For steady experiments, each operating point was sampled over 8s to ensure reasonable averaged results. The results of transient experiments were filtered using Savitzky-Golay FIR filter, including the flow discharge, the torque, and the pressure in spiral case and draft tube. It is based on polynomial fitting of the raw data, extracting the time-averaged pressure based on the least squares method [17]. The filtered flow parameters should be smooth enough, so a third-order Savitzky-Golay FIR filter with a frame size of 1.0 s was selected. The performance curves in pump mode were described for pump mode with Equation.1.

$$E_{nD} = \frac{E}{n^2 D^2} \quad Q_{nD} = \frac{Q}{nD^3} \quad T_{nD} = \frac{T}{\rho n^2 D^5} \tag{1}$$

3.1. Steady performance

3.1.1. General performance. To begin with, the influence of GVO on the global performance parameters should be evaluated. Therefore, the general performance of the unit under different GVOs had been obtained in nominal rotational speed of the unit, 1000 rpm, as was shown in figure 3. According to Equation.2, the flow and torque were normalized with maximum value, while the head was normalized with nominal value. It was observed that the effect of the GVO on the head was rather small. The maximum value of flow, torque and efficiency (79%) occurred under guide blade opening 16.9 *deg*, which was considered to be the best efficiency opening in the pump mode. Spherical valve regulation would be used to investigate the performance of this opening. In addition, another two openings, 10 *deg* and 23 *deg* were also selected for comparison.

$$y = \frac{y(\alpha)}{y_{ref}} \tag{2}$$

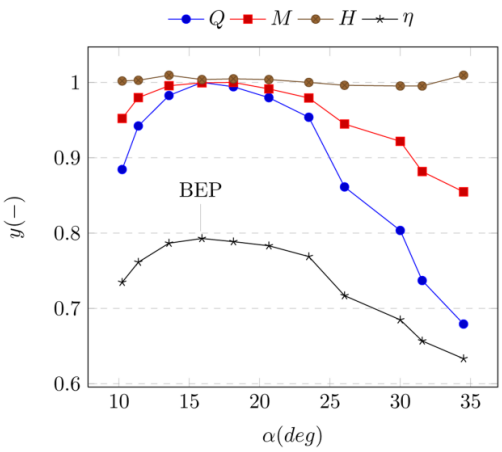

Figure 3. Global performance of the pump-turbine for different GVOs

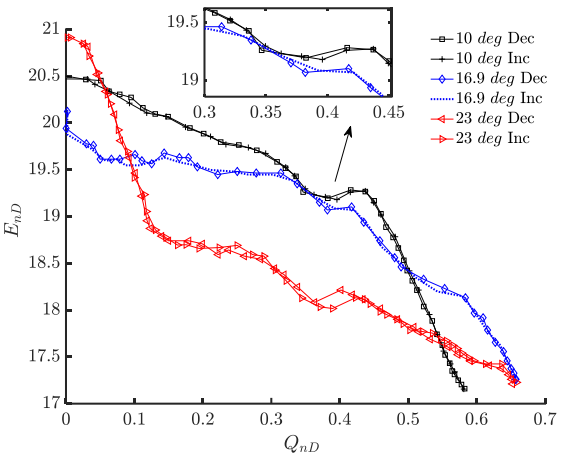

Figure 4. Performance curves of energy coefficient for three GVOs by increasing/ decreasing the opening of the spherical valve

3.1.2. Detailed investigation. In order to further study the pump performance under fixed GVOs, meticulous point-to-point steady measurements were completed by adjusting the spherical valve opening. Due to the ability of the grid, the variation of rotational speed was kept within 0.2% even in deep part flow conditions. Under each GVO, experiments were conducted including flow decreasing direction as well as flow increasing direction. The performance of energy, torque, efficiency, and characteristics of hysteresis, pressure pulsations would be discussed.

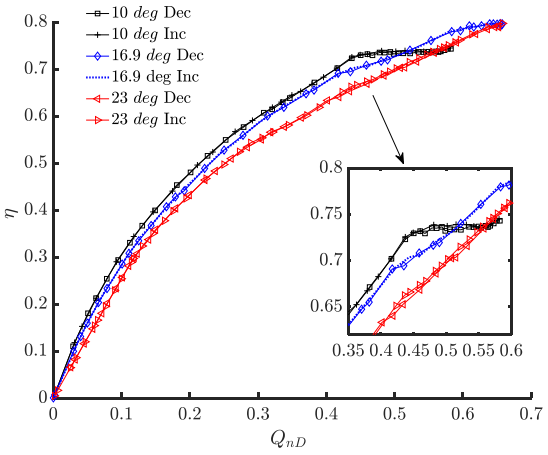

Figure 4.b Performance curves of efficiency for three GVOs by increasing/ decreasing the opening of the spherical valve

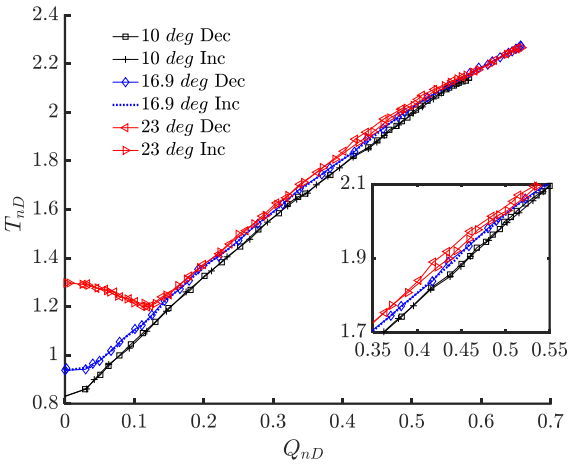

Figure 4.c Performance curves of torque coefficient for three GVOs by increasing/ decreasing the opening of the spherical valve

Figure 4 presented the performance curves of energy coefficient, efficiency, and torque coefficient under three GVOs in flow decreasing direction and flow increasing direction. It was founded that the drop of energy performance was significant from Q_{nD} = 0.35 to Q_{nD} = 0.4, which was called the hump characteristics. Besides, the hysteresis of energy performance caused by flow variation direction was obvious from Q_{nD} = 0.35 to Q_{nD} = 0.4 in a large GVO, 23 *deg*. However, for lower GVOs, the repeatability of the performance curves was satisfactory and the hysteresis was not clear. It should be mentioned that due to limited variation of water level in the upstream reservoir and downstream

reservoir, performance curves of the unit in pump mode could only be partially obtained by steady measurements.

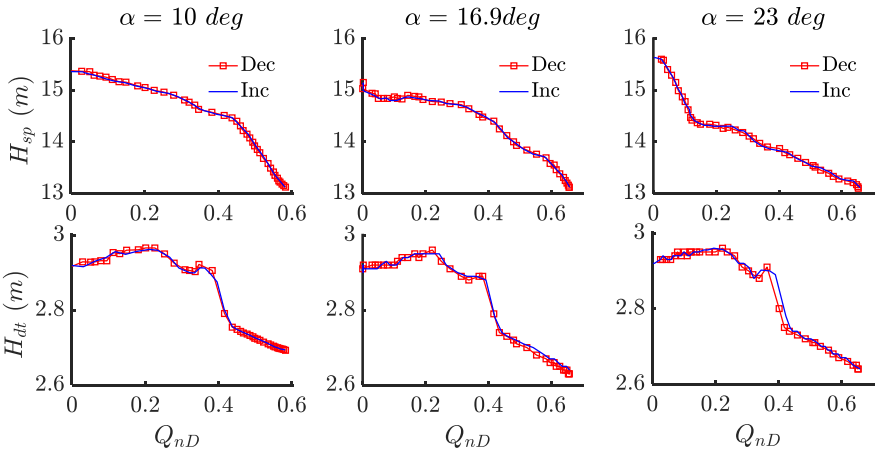

Figure 5. Variation of pressure in spiral case and draft tube versus flow coefficient of three GVOs

To identify the cause of the drop in energy performance, figure 5 displays the variation of pressure in spiral case and draft tube versus flow coefficient of three GVOs. It was observed that the pressure in spiral case varied monotonously in part flow conditions. However, the pressure in draft tube under three GVOs increased sharply around QnD = 0.4 and then dropped, which was the cause of the sudden drop of energy coefficient. In addition, hysteresis of draft tube pressure was witnessed under GVO 23 deg. In contrast, pressure in spiral case showed no difference in flow decreasing direction or in flow increasing direction. This indicated that the hysteresis of energy performance in pump mode came from the inlet of draft tube.

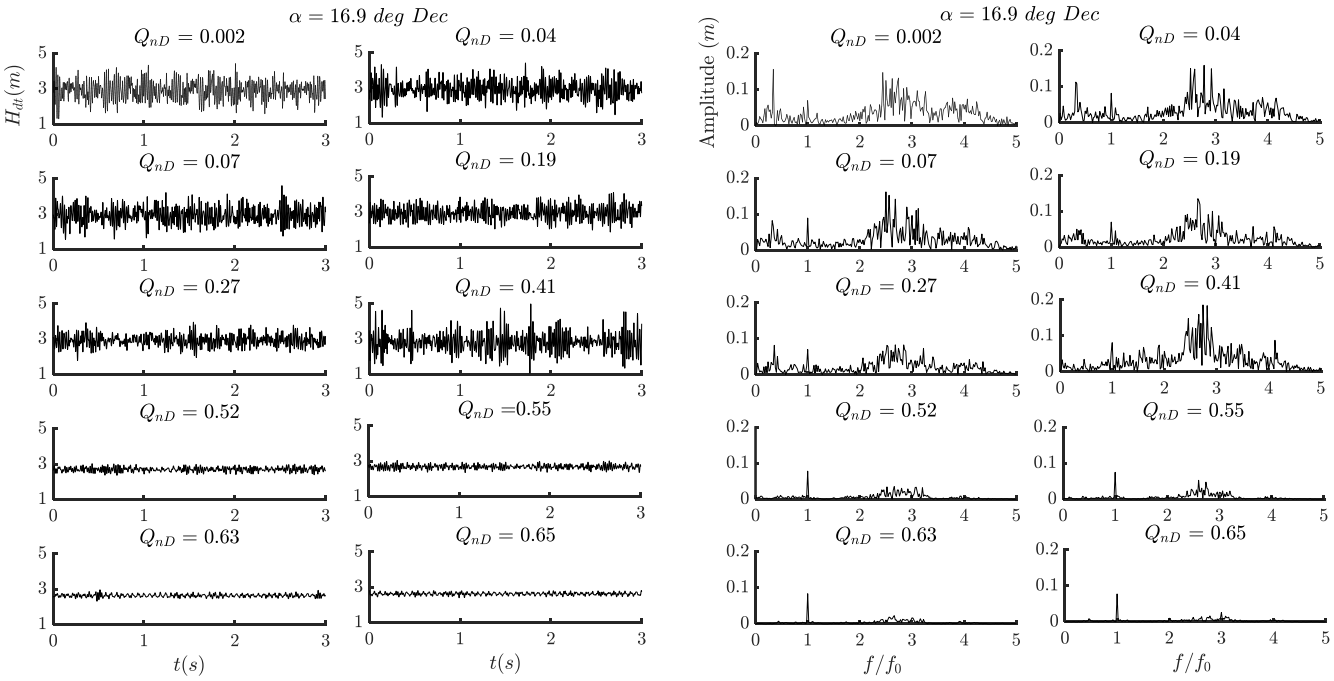

Figure 6. Pressure pulsations in draft tube in time domain (left) and frequency domain (right) for 16.9 *deg* GVO, flow decreasing direction

Analysis of pressure pulsations were conducted with ten selected steady operating points from a GVO of 16.9 deg in flow decreasing direction. Figure 6 shows the absolute value of pressure pulsations in draft tube in both time and frequency domain. From the view in time domain, the amplitude of pressure pulsations did not vary significantly until Qnd = 0.41. As with the further decrease of the flow, the amplitude became lower when Qnd = 0.27. It could be also observed from frequency domain that the amplitude of frequencies between 2f0 and 3f0 gradually became intense and reached maximum at Qnd = 0.41. Despite the source of these frequencies might not be determined accurately, it was sure that they were related to the flow patterns in the draft tube.

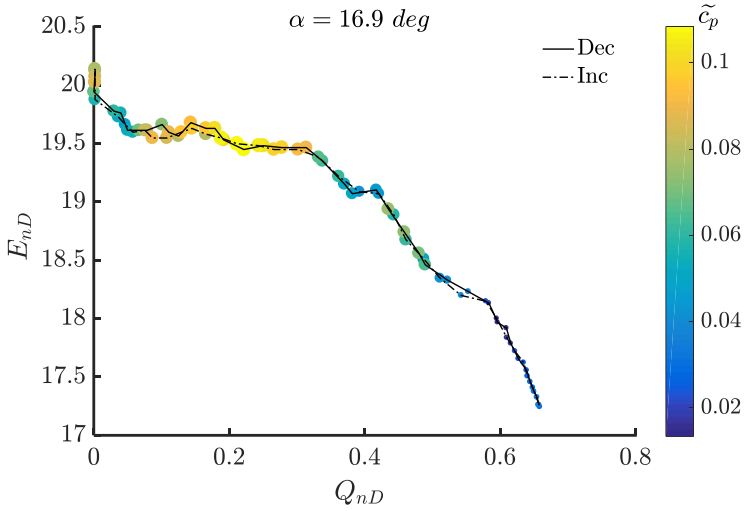

Figure 7. Pressure coefficient of pressure pulsations in the vaneless region for 16.9 *deg* GVO

Figure 7 illustrates the pressure coefficient of pressure pulsations in the vaneless region between the runner and the guide vane for 16.9 deg GVO in both flow decreasing direction and flow increasing direction. The pressure coefficient representing the standard deviation of pressure pulsations was calculated with equation (3). It was observed that the pressure coefficient in the vaneless region gradually increased when QnD was lower than 0.55. The maximum value of pressure coefficient, 0.13, was located at QnD= 0.22. Hysteresis of pressure coefficients in the vaneless region was not significant.

$$\tilde{C}_p = \frac{1}{\rho E}\sqrt{\frac{1}{N}\sum_{i=1}^{N}(p_i - \bar{p})^2} \tag{3}$$

Pressure pulsations in the vaneless region were normalized with Equation.4 and shown in figure 8 in time and frequency domain.

$$C_p = \frac{p - \bar{p}}{\rho E} \tag{4}$$

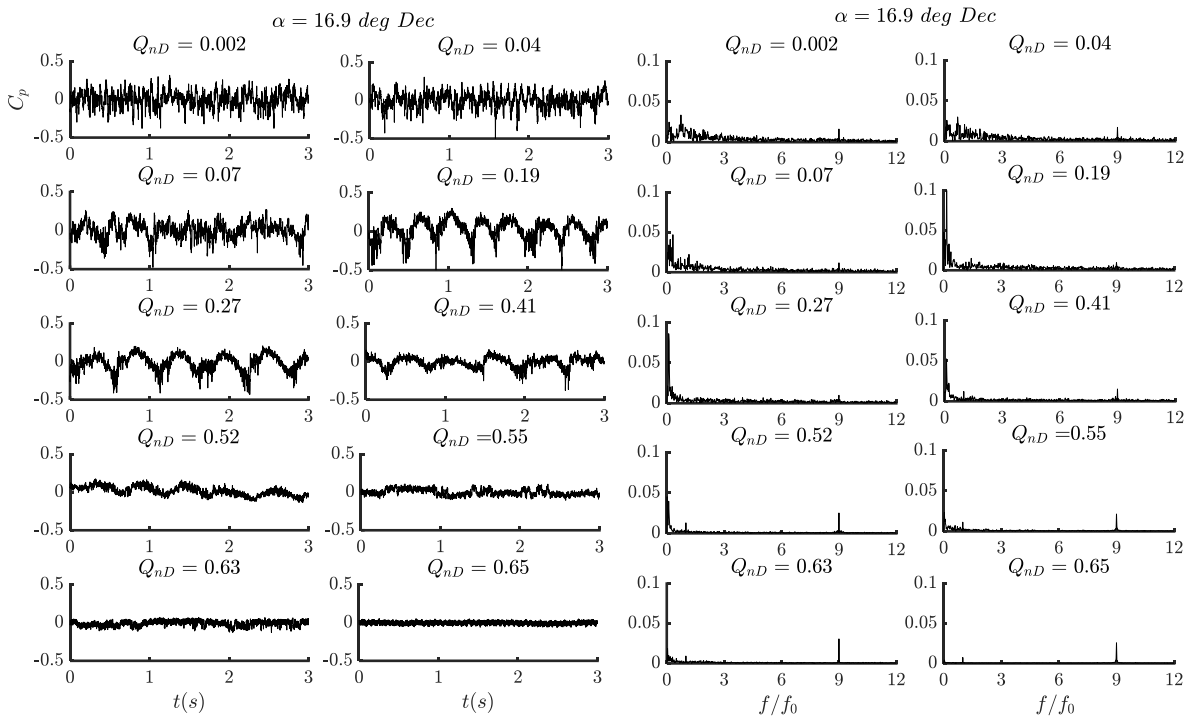

Figure 8. Pressure pulsations in vaneless region in time domain and frequency domain for 16.9 *deg* GVO, flow decreasing direction

Initially, when QnD = 0.65, it was observed that the blade passing frequency 9 f0 dominated the frequency domain. However, a frequency of 0.1 f0 became visible in frequency domain as QnD decreased to 0.52. The intensity of the amplitude at this frequency rose gradually and became dominant in frequency domain as QnD decreased to 0.27. Meanwhile, pressure pulsations in time domain clearly indicated a shape of strong periodic low frequency. It was also found that when QnD reached 0.19, the frequency of periodic pressure pulsations varied slightly from 0.1 f0 to 0.16 f0. From QnD = 0.19 to 0, the amplitude of 0.16 f0 became lower and blade passing frequency 9 f0 could be observed again.

Results from steady experiments showed that, in part flow conditions QnD = 0.41, it was the flow pattern in draft tube cone that resulted in the sudden drop of performance curves. On the one hand, the averaged pressure in draft tube appeared a sudden increase, making the energy performance curves hump shaped. On the other hand, the amplitude of the pressure pulsations in draft tube experienced a sudden rise in partial flow condition, indicating the complex flow patterns. In addition, as the QnD decreases from 0.65 to 0.52, pressure pulsations in the vaneless region became intense both in time and frequency domain. But it was clear that no significant change in the vaneless region was observed as either in time domain or in frequency domain from QnD = 0.52 to QnD = 0.41, which was in contrast with pressure characteristics in draft tube. Thus it can be concluded that pressure pulsations between runner and guide vane were not the direct cause for the hump characteristics.

3.2. Transient performance

3.2.1. Continuous closing/opening of the spherical valve. As was discussed before, steady point-to-point measurements were conducted by regulating the opening of the spherical valve. However, this method of static measurement was time-expensive. Besides, the authors were motivated by similar work of Hasmatuchi [18], who performed dynamic measurements of hydraulic efficiency in turbine mode by increasing or decreasing the speed of the turbine. Therefore, dynamic experiments to acquire performance curves with continuous of regulation spherical valve were carried out to test the

feasibility of dynamic measurements. The spherical valve was controlled to switch from the 100% opening to 0 opening with the switch time T_s = 6s, 10s and 30s respectively. During this period, the rotational speed was kept constant by the grid. As reference, performance curves obtained in steady experiments were also presented. Figure 9 shows the performance curves acquired by continuous regulation of the spherical valve under 16.9 *deg* GVO. Each dynamic test was plotted with a repeated test.

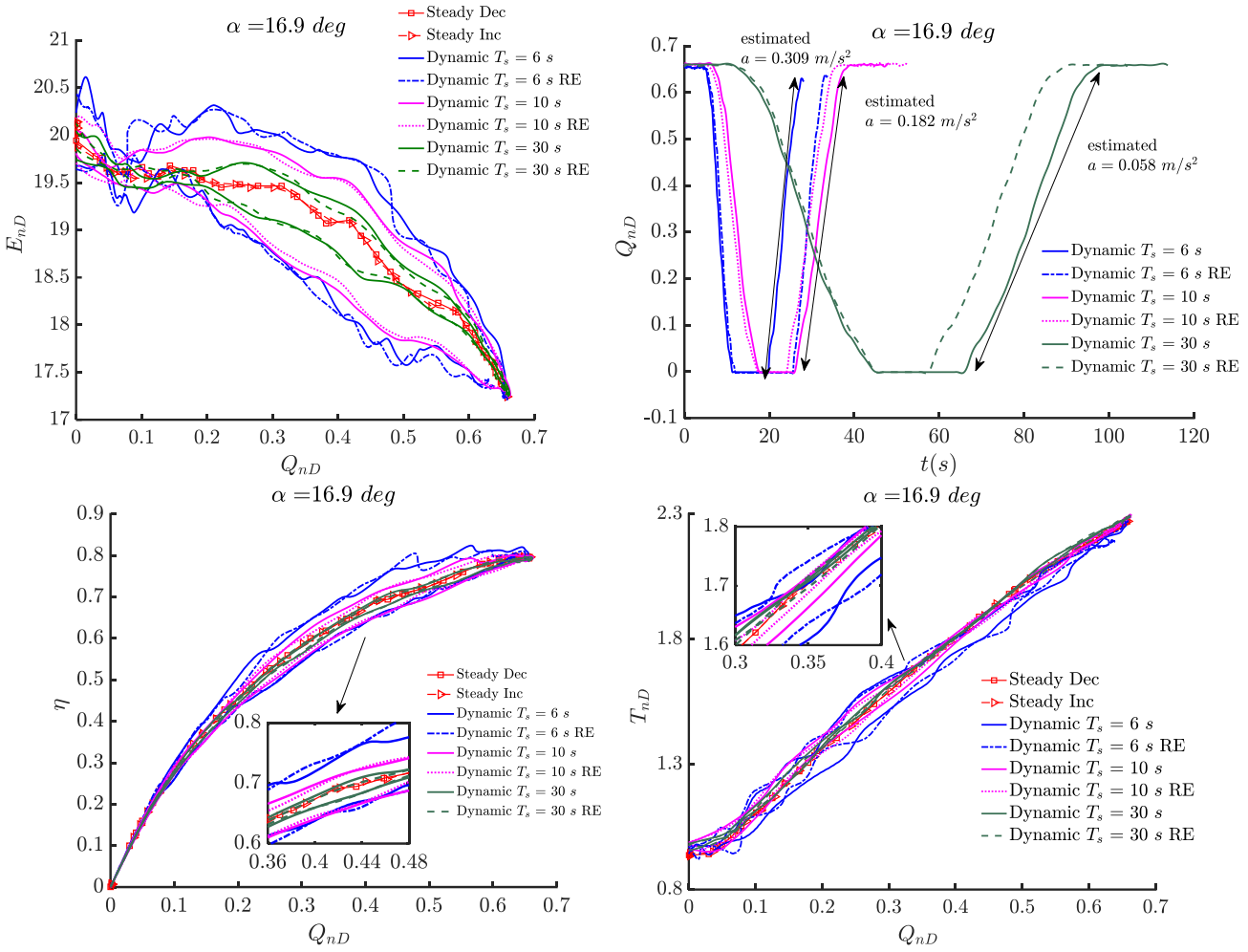

Figure 9. Performance curves acquired by dynamic tests with continuous regulation of the spherical valve

$$a = \frac{1}{A}\frac{dQ}{dt} \tag{5}$$

The flow acceleration under different switch time was estimated with Equation.5. For the switch time Ts = 6s, 10s and 30s, the estimated flow acceleration a was 0.309 m2/s、0.182 m2/s、0.058 m2/s, respectively. It was observed that the dynamic loop was most significant when Ts = 6s. With Ts increasing, the dynamic loop became small and approached the steady performance curves. Especially, the results from dynamic tests and steady tests for efficiency performance and torque performance were almost coincident when Ts = 30s, while the dynamic loop of the energy performance curve was still obvious. Therefore, the dynamic experiment with switch time Ts = 30s and flow acceleration a = 0.058 m2/s could be utilized for the measurement of the performance curves of efficiency and torque in a quasi-steady way.

3.2.2. Extension of pump performance curves with a transient method. In the previous steady tests, it was not sure whether the highest efficiency of the pump turbine in pump mode had been achieved. Since the water level was constant either in the upstream reservoir or in the downstream reservoir, performance curves acquired by the steady experiments were limited. In order to extend the performance characteristics towards higher Q_{nD} region, a unique method for open loop test rigs was proposed. First, the water level in both upstream and downstream was maintained at nominal value. Then, the circulating pump which delivers water from underground to both upstream and downstream was shut. The head across the model pump turbine would gradually decrease from designed value due to gravity. When the head dropped to a value which was sufficient low, for example 40% designed head, the unit would be started in pump mode to operate at a given GVO. In this way, the net head would be increased by the pump-turbine through delivering water from the downstream reservoir to fill up the upstream reservoir. Before the upstream reservoir was full, there would be a period which could be used for transient measurement of the performance curve.

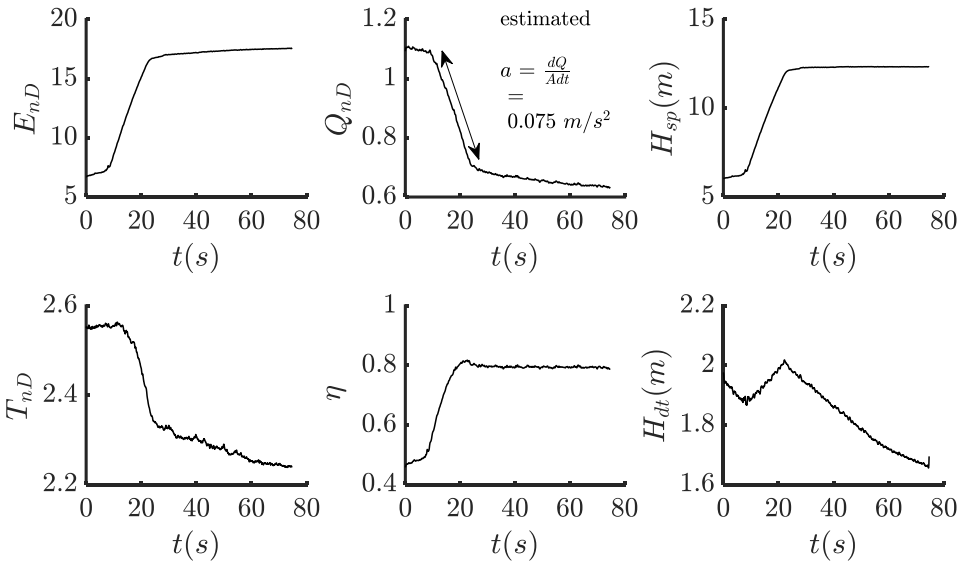

Figure 10. Variation of flow parameters from the first transient test for 16.9 *deg*

For a preliminary investigation, the GVO 16.9 deg was selected. Transient experiments with the proposed method were conducted three times. The variation of flow parameters from the first transient test were presented in figure 10. It can be seen that the pressure in spiral case increased just as the shape of upstream pipe shown in figure 1, indicating that the water was pumped to the upstream in this process. The absolute value of maximum flow acceleration during transient tests was estimated as 0.075 m2/s for Transient 1, 0.072 m2/s for Transient 2, and 0.068 m2/s for Transient 3. For comparison, performance curves acquired by all three transient tests were plotted with steady performance curves in figure 11. It was observed that the results of proposed transient tests could be utilized qualitatively to extend the performance curves. The maximum efficiency under 16.9 deg was obtained as 82% in Transient 1. However, the repeatability of this transient test was not good, and the juncture between steady tests and transient tests could not be precisely identified. The reason was that this was a spontaneous, uncontrollable transient process in which the flow motion was related to not only geometry of the upstream pipe, but also instantaneous head when the pump-turbine started to operate in pump mode.

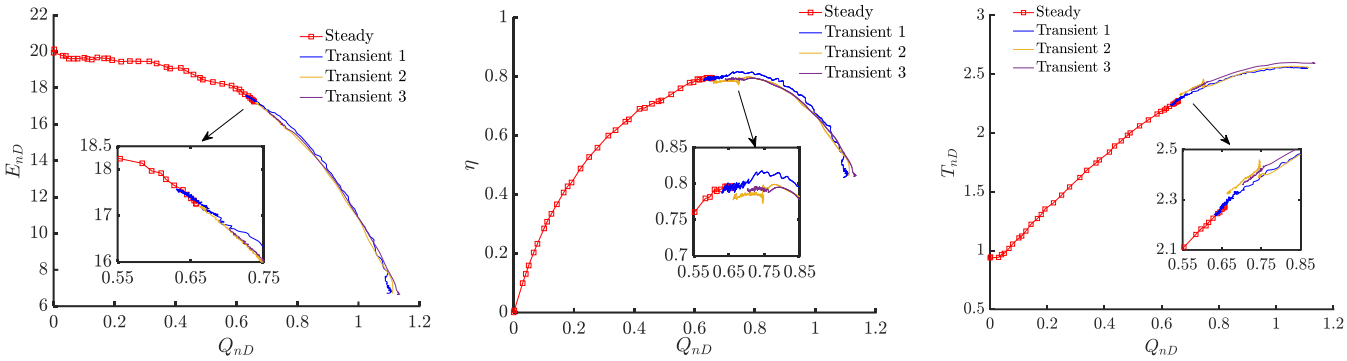

Figure 11. Performance curves acquired all three transient tests for 16.9 *deg*

4. Conclusions

To get a better understanding of pump performance of a model pump-turbine, detailed experiments have been conducted on an open-loop test rig, including steady tests and transient tests. The results are concluded in the following:

- A sudden change of pressure in draft tube is the cause of hump shaped characteristics as well as hysteresis of energy performance curves.
- The efficiency and torque performance curves in pump mode could be feasibly measured by continuous closing or opening the spherical valve if the switch time is sufficient long.
- The performance curves were dynamically obtained by a spontaneous operation of the pump-turbine in low head, while repeated tests show that the juncture between steady tests and transient tests could not be precisely identified.

The precise measurement of flow discharge in fluid transients is of great significance. However, currently electromagnetic flow meter was used in transient investigations, whose response to fast variation of flow discharge was generally weak. This was a source of error for dynamic measurements of performance curves. In addition, the selection of parameters for dynamic filtering is a factor for error. These influences should be considered in further investigations.

Acknowledgments

This work was supported by the National Natural Science Foundations of China (Grant No. 51039005). In addition, the authors would like to acknowledge the contribution from the lab's technical staff, especially Mr Xuewu Wang， Mr Bin Liu and Ms Lihua Sun.

References

[1] Ran H, Luo X, Lei Z 2012 Experimental Study of the Pressure Fluctuations in a Pump Turbine at Large Partial Flow Conditions. *Chinese Journal of Mechanical Engineering*, 2012, 25(6):1205-1209.

[2] Ješe U, Skotak A, Mikulašek J. Cavitating vortices in the guide vanes region related to the pump-turbine pumping mode rotating stall, *IAHR International Meeting of the Workgroup on Cavitation and Dynamic Problems in Hydraulic Machinery and Systems* 2017:012043.

[3] Yang J, Pavesi G, Yuan S, et al. Experimental Characterization of a Pump–Turbine in Pump Mode at Hump Instability Region, *Journal of Fluids Engineering*, 2015, 137(5).

[4] Lu G, Zuo Z, Sun Y, et al. Experimental evidence of cavitation influences on the positive slope on the pump performance curve of a low specific speed model pump-turbine, *Renewable Energy*, 2017.

[5] Zhang Z 2010 *IOP Conf. Ser.: Earth and Environ. Sci*. 12 012010

[6] Braun O 2009 Part Load Flow in Radial Centrifugal Pumps PhD Thesis EPFL

[7] Guggenberger M, Senn F, Jaberg H, et al. Experimental analysis of the flow pattern of a pump turbine model in pump mode, IOP Conference Series: Earth and Environmental Science. *IOP Conference Series: Earth and Environmental Science*, 2016.

[8] Edinger G, Erne S, Doujak E, et al. Flow determination of a pump-turbine at zero discharge, IOP Conference Series: Earth and Environmental Science. *IOP Conference Series: Earth and Environmental Science*, 2014:032051.
[9] Anciger D, Jung A and Aschenbrenner T 2010 *IOP Conf. Ser.: Earth and Environ. Sci*. 12 012013
[10] Li D, Wang H, Qin Y, Wei X, and Qin, D. (2017). Numerical simulation of hysteresis characteristic in the hump region of a pump-turbine model. *Renewable Energy*.
[11] Zhang X, Burgstaller R, Lai X, Gehrer A, Kefalas A, and Pang Y. (2016). Experimental and Numerical Analysis of Performance Discontinuity of a Pump-Turbine under Pumping Mode. IOP Conference Series: Earth and Environmental Science (Vol.49, pp.042003). *IOP Conference Series: Earth and Environmental Science*.
[12] IEC 60193: 1999-11, Hydraulic Turbines, Storage Pumps and Pump-Turbines—Model Acceptance Tests, International Electrotechnical Commission, Geneva, Switzerland.
[13] Doerfler P K, Engineer A J, Pendse R N, et al. Stable operation achieved on a single-stage reversible pump-turbine showing instability at no-load, *IAHR Section Hydr. Machinery and Cavitation, Symposium*, 1998.
[14] Landry C, Alligné S, Hasmatuchi V, Roth S, Mueller A, and Avellan F (2011). Non-Linear Stability Analysis of a Reduced Scale Model Pump-Turbine at Off-Design Operation. *IAHR International Meeting on Cavitation and Dynamic Problems in Hydraulic Machinery and Systems*.
[15] Nielsen T, Fjørtoft Svarstad M, Unstable behaviour of RPT when testing turbine characteristics in the laboratory, *IOP Conference Series: Earth & Environmental Science* 2014:032038.
[16] Guggenberger, M, et al. ,Investigating the dynamic aspects of the turbine instability of a pump turbine model, *IAHR International Meeting of the Workgroup on Cavitation and Dynamic Problems in Hydraulic Machinery and Systems* 2015.
[17] Schafer R W, What is a Savitzky-Golay filter, *IEEE Signal Processing Magazine*, 7(2011) 111-117.
[18] Hasmatuchi V, Bosioc A, and Münchalligné C. (2016). On the Dynamic Measurements of Hydraulic Characteristics. *IOP Conference Series: Earth and Environmental Science* (Vol.49, pp.062001). IOP Conference Series: Earth and Environmental Science.